Dual-energy computed tomography in the diagnosis of mediastinal tumor

Suyon Chang

Department of Medicine

The Graduate School, Yonsei University

Dual-energy computed tomography in the diagnosis of mediastinal tumor

Directed by Professor Jin Hur

The Master's Thesis
submitted to the Department of Medicine,
the Graduate School of Yonsei University
in partial fulfillment of the requirements for the degree
of Master of Medical Science

Suyon Chang

June 2014

This certifies that the Master's Thesis of
Suyon Chang is approved.

Thesis Supervisor : Jin Hur

Thesis Committee Member#1 : Hye-Jeong Lee

Thesis Committee Member#2 : Dae Joon Kim

The Graduate School
Yonsei University

June 2014

ACKNOWLEDGEMENTS

I acknowledge my deep gratitude to Professor Jin Hur, who is my thesis director, for supporting my efforts with total commitment and facilitating every step of the process. My appreciation for his guidance and encouragement is tremendous. I am also indebted to Professor Hye-Jeong Lee and Dae Joon Kim, for their help for pertinent advice to assure the superior quality of this paper.

<TABLE OF CONTENTS>

LIST OF FIGURES

LIST OF TABLES

ABSTRACT

Dual-energy computed tomography in the diagnosis of mediastinal tumor

Suyon Chang

Department of Medicine

The Graduate School, Yonsei University

(Directed by Professor Jin Hur)

PURPOSE: The purpose of this study is to investigate the diagnostic utility of dual-energy computed tomography (DECT) in differentiating between mediastinal 1) cystic and solid masses, and 2) benign and malignant tumors.

MATERIALS AND METHODS: Our institutional review board approved this study, and patients provided informed consent. We prospectively enrolled 38 patients (18 males; mean age: 46 years) who had suspected mediastinal tumors on chest radiography or chest computed tomography (CT). All patients underwent a DECT using gemstone spectral imaging (GSI) mode (GE HD750). For qualitative

analysis, each mass was characterized in terms of its size, location, internal characteristics, and external characteristics. For the quantitative analysis, two reviewers measured the following parameters of the tumors: CT attenuation value in Hounsfield units (HU), iodine-related HU, and iodine concentration (mg/ml). Pathological results were used for a final diagnosis. Statistical analyses were performed using the Fisher's exact test, independent samples t-test, and Mann-Whitney test.

RESULTS: In qualitative analysis, malignant tumors were more likely to be greater in size ($p = 0.015$), with lobulated or irregular contours ($p < 0.001$), a necrotic or cystic component ($p = 0.025$), local invasion ($p < 0.001$), metastasis ($p = 0.016$), and lymphadenopathy ($p < 0.001$) than were benign tumors. In comparison of mediastinal cysts and masses, the mean attenuation values in HU, iodine-related HU, and iodine concentration were higher in mediastinal masses than cysts (all $p < 0.001$). In comparison of benign and malignant tumors, the iodine related HU was significantly lower in malignant tumors than benign tumors ($p = 0.041$).

CONCLUSION: DECT using a quantitative analytic method based on iodine concentration measurements can be used to evaluate tumor enhancement of medistinal tumors using a single-phase scanning. Therefore, we believe that DECT could be a helpful complementary tool in cases where conventional contrast CT is inconclusive.

Key words: mediastinal neoplasms, dual-energy computed tomography, differentiation, benign neoplasm, malignant neoplasm, cyst

Dual-energy computed tomography in the diagnosis of mediastinal tumor

Suyon Chang

Department of Medicine

The Graduate School, Yonsei University

(Directed by Professor Jin Hur)

I. INTRODUCTION

Mediastinal masses span a wide histopathological and radiological spectrum. Mediastinal space is divided into several compartments, but there are no physical boundaries between compartments that limit disease. Anterior mediastnal masses include retrosternal goiter, thymic tumor, germ cell tumor, pleuropericardial cyst, lymphatic malformation, and hemangioma. Middle mediastinal masses include foregut duplication cyst,

such as bronchogenic, esophageal, or neurenteric cyst. Posterior mediastinal masses include neurogenic tumor, foregut duplication cyst, paraspinal abscess, and lateral meningocele.[1]

The diagnostic imaging is important because of the different therapeutic strategies used to treat these lesions. Some asymptomatic benign lesions such as pericardial cysts can be followed expectantly. When they are causing symptoms, percutaneous aspiration, ethanol sclerosis, or resection can be performed.[2] Patients who were suspected for secondary neoplasms or lymphoma may need diagnostic biopsy for confirmation and/or subclassification. Patients with lymphoma or small cell lung carcinoma would be treated by cytotoxic chemotherapy rather than surgery.[3] Patients with mediastinal lesions that are suitable for complete resection with low risk of operation may undergo surgical resection without biopsy. In thymoma, imaging can preoperatively distinguish the patients who require neoadjuvant chemotherapy (ie, patients with more advanced thymomas) from those who do not (ie, patients with early disease).[4]

For the radiologic diagnosis of mediastinal masses, computed tomography (CT) is generally the first choice modality of diagnostic imaging. Multi-detector CT provides high-resolution multiplanar

reformation images display the detailed anatomical relationship of the tumor with the adjacent structure. CT enables us to evaluate the size, morphology, location, and extent of the mediastinal masses.[5] While relatively specific imaging clues exist for certain lesions such as teratoma and cysts, many solid malignant and benign masses appear remarkably similar on CT. Although, we can measure the attenuation of the X-ray beam (Hounsfield unit (HU)) through the lesion to characterize it, CT may reveal high attenuation similar to solid lesions in some mediastinal cysts due to a high level of protein and calcium oxalate in the cystic contents. Thymic cysts with hemorrhage or inflammation may show attenuation equal to the muscle on CT which mimic solid tumors. Bronchogenic cysts can also contain various amounts of protein and calcium and therefore can mimic solid tumors.[6]

Magnetic resonance imaging (MRI) can provide additional information for diagnosis owing to its excellent soft tissue resolution. It is useful in confirming the cystic nature of mediastinal lesions that appear solid at CT.[7] In addition to conventional T1- and T2- weighted images, dynamic study, chemical shift images and diffusion-weighted images (DWI) can be used. Dynamic multiphase gadolinium-enhanced study is useful in the assessment of vascularity and extracellular space volume of the lesions.

Chemical shift MRI detects fatty infiltration within the thymus, and is useful to differentiate thymic hyperplasia from thymic neoplasms. Apparent diffusion coefficient (ADC) measurement on DWI may be also helpful in differentiating malignant from benign mediastinal masses. Despite the introduction of many techniques to overcome motion artifact, the motion of structures induced by heart pulsation and respiration has been the major problem of MRI. Susceptibility artifacts associated with echo-planar imaging sequences can be another limitation.[5,8] Moreover, it is often not available because it requires high cost and relatively long acquisition time, and some patients with certain ferromagnetic implants or claustrophobia cannot be studied. On the other hand, CT has been most often used due to its wide availability and cost-effectiveness.

Since angiogenesis is essential for tumor growth, an enhanced vascular supply can reflect a malignant potential.[9,10] It is known that there is a significant correlation between tumor angiogenesis and invasiveness in thymic epithelial tumors.[10] There have been efforts to differentiate benign from malignant pulmonary nodules with CT. Blood supply and metabolism of malignant pulmonary nodules are proved to be different from most benign nodules.[11] The extent of enhancement at dynamic CT is known to reflect the underlying extent of nodular angiogenesis, and

several studies reported various threshold attenuation values for the differentiation between benign and malignant nodules.[12-14] Yamashita et al. reported that a maximum attenuation of 20–60 HU appears to be a good predictor of malignancy[12], and Swensen et al. suggested 15 HU as a threshold value for predicting benignity.[13] In a dynamic study with multi–detector row CT, higher peak enhancement was obtained, and with a cutoff value of 30 HU of net enhancement overall diagnostic accuracy was similar to that in previous studies.[14] Analyzing combined wash-in and washout characteristics at dynamic multi–detector row CT or analyses of wash-in values plus morphologic features during helical dynamic CT scanning can be also useful for the characterization of the nodule.[15,16] However, contrast-enhanced dynamic CT has some disadvantages. It requires repeated scans leading to large amount of radiation exposure. Also, measurement can be inaccurate due to different positioning of the regions of interest (ROIs) on serial images of dynamic scanning.[17] In addition, the CT number in HU merely represents different density levels of tissues and other substances. HU values can be influenced not only by iodine contrast delivered by the vascular system, but also by the presence of dense material containing blood, protein or calcification.

Recently introduced dual-energy CT (DECT) is known to offer a specific tissue characterization and improve the assessment of vascular disease. CT numbers of materials with high atomic numbers vary with beam energy, so materials can be differentiated by applying different X-ray spectra. Iodine is one of those materials and is known to have stronger enhancement at lower tube voltage. This enables differentiating iodine from other materials that do not show this behavior. DECT can transform the attenuation measurements into the density of water and iodine, which is so called material decomposition. As iodine is commonly used in CT as a contrast material, quantification of iodine enables us to measure the vascular enhancement of the lesion, and it may be applied for differentiating complicated cysts from solid tumors.[18] Therefore, we hypothesized that iodine concentration measurements with DECT data would provide a more reliable quantitative parameter to indicate tumor enhancement that could help radiologists differentiate between solid masses and complicated cysts, and between benign and malignant mediastinal tumors.

The purpose of this study is to investigate the diagnostic utility of DECT in differentiating between mediastinal 1) cystic and solid masses, and 2) benign and malignant tumors.

II. MATERIALS AND METHODS

1. Patient selection

This single-center prospective study was approved by our institutional review board, and informed consent was obtained from all patients. From September 2012 to April 2014, 62 patients who have a suspected mediastinal tumor on chest radiography or chest CT were enrolled to undergo DECT after meeting our inclusion criteria. We got informed consent from all patients. Our inclusion criteria were as follows: (a) a mediastinal mass excluding typical thyroid masses and vascular lesions; (b) lesions >10mm in diameter based on the longest diameter between the long and short axes; (c) no use of previous chemotherapeutic or radiotherapeutic treatments. Fifteen patients were excluded from this study according to the exclusion criteria, as follows: (a) No true mediastinal tumor (n=8); (b) Lack of pathologic results (n=16). As a result, 38 patients (18 males; mean age: 46 years) were ultimately enrolled in this study.

2. Dual-energy computed tomography examination

DECT scans were performed with a 64-row multidetector CT scanner (Discovery CT750 HD; GE Healthcare, USA). Images were acquired during a single breath-hold from the lung apex to the costophrenic angles in the cranio-caudal direction. The scan delay was determined using a test bolus method. A test bolus was performed with an injection of 10 ml of contrast agent, iopamidol (300 mg of iodine per milliliter; Radisense, Tae-joon Pharm, Seoul, Korea), followed by 30 ml of normal saline at 3 ml/s. The time to peak enhancement in the main pulmonary artery (PA) was determined using the resultant time-enhancement curve. The scan was obtained 60 s after peak enhancement of the main PA. For contrast enhancement, 50-90 ml (1 ml/kg) of iopamidol (300 mg of iodine per milliliter; Radisense, Taejoon Pharm, Seoul, Korea) was injected at 3 ml/s, followed by a 20 ml saline chaser also at 3 ml/s. We used a fast switched spectral CT in gemstone spectral imaging (GSI) mode (DECT mode), in which the energy of the X-ray beam rapidly switches. The scan parameters were as follows: detector collimation, 64 mm × 0.625 mm; gantry rotation time, 0.5 s; tube voltage, 140 and 80 kV; tube current, 630 mAs; and pitch, 1.375:1. All images were reconstructed with a slice thickness of 1.25 mm with a detail reconstruction kernel, and data were transferred to an off-line workstation (GE workstation, Volumeshare 5,

GE Healthcare, USA). Dual energy CT X-ray projection data were transformed into images representing a range of monochromatic X-ray images (40–140 keV) in increments of 1 keV to form material basis pair images including water (iodine), iodine (water), and effective atomic number (Z) that the user could interactively change depending on the needs. The calculated mean radiation dose was 5.95 mSv (DLP range, 134 to 489 mGy*cm) depending on the scan range.

3. Imaging analysis

CT data were analyzed by two radiologists and both were blinded to patient identities and clinical histories. All scans were processed and read using a dedicated workstation equipped with dual-energy post-processing software (GE workstation, Volumeshare 5, GE Healthcare, USA).

For the qualitative analysis, each mass was characterized in terms of its size (longest diameter between the long and short axes), location (anterior, middle and posterior mediastinum), internal characteristics (contour, necrotic or cystic component, calcification) and external characteristics (local invasion, metastasis, pericardial or pleural effusion, lymphadenopathy).

For the quantitative analysis of enhancement, the reviewers measured the mean CT attenuation value of the mediastinal tumors in Hounsfield units (HU) at three slices, selected independently by the two reviewers, among the virtual monochromatic 70 keV images, synthesized from DECT data, that are known to be similar to conventional 120 kV images. The mean HU of the mediastinal tumors was used for analyses. On post-contrast CT images, a region of interest (ROI) was drawn within the mediastinal tumors to be as large of an area as possible. The reviewers also measured the mean CT attenuation value of the mediastinal tumors in HU with material suppressed iodine (MSI) images provided by the workstation. The MSI images were used to measure HU that were to approximate those of non-enhanced 120 kV images to calculate the mean iodine-related HU (IHU) of the mediastinal tumors. The mean iodine-related HU (IHU) was calculated as follows: IHU = post enhanced HU − non-enhanced HU. The reviewers also measured the iodine concentration of the mediastinal tumors with the iodine (water) images provided by the workstation. The two reviewers independently measured iodine concentrations (mg/ml) on the same slice with which HU was measured; averaged values were used for analysis. The three modes of images, monochromatic 70 keV images representing

post-contrast CT images, MSI images representing pre-contrast CT images, and iodine (water) images could be displayed on the workstation, side by side at the same time, linked together, therefore demonstrating identical level of the mediastinal tumor for each mode (Figure 1).

(A) (B)

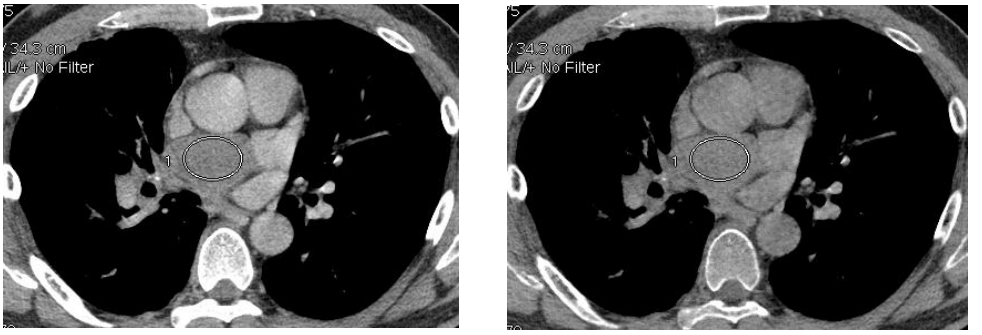

(C)

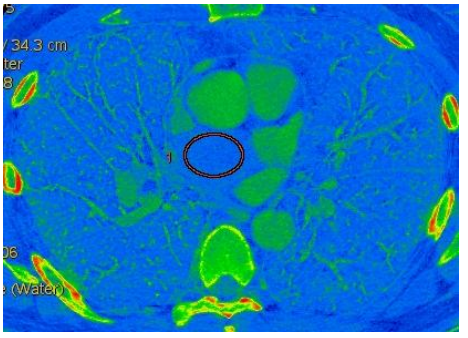

Figure 1. Example of image set of a patient with a middle mediastinal lesion. Three modes of images obtained by dual-energy CT data, (A) monochromatic 70 keV image representing post-contrast CT image, (B) MSI image representing pre-contrast CT image, and (C) iodine (water) image demonstrating identical level of the mediastinal tumor were displayed on the workstation.

The iodine (water) images were used to quantitate the concentration of iodine based on the following process. First, the attenuation of X-rays of a single energy, E, through two known materials, m1 and m2 (with densities d1 and d2, respectively), can be computed using the equation below:

$$p = -\ln\left(\frac{I}{I0}\right) = d1\mu1(E) + d2\mu2(E).$$

The calculation of the monochromatic image is a linear operation performed on the material basis images and is normalized to water to ensure that the attenuation of water is consistent with that of the polychromatic images, where water is assumed to be material m1.

$$I = I0e^{-(\mu1(E)d1+\mu2(E)d2)},$$

This equation describes how the material density images are transformed to a monochromatic image at energy E, where I0 is the incident radiation, I is the transmitted radiation, $\mu1(E)$ and $\mu2(E)$ are the X-ray attenuation coefficients at a specific energy level E, and d1 and d2 are the material densities in milligrams per milliliter of the material density pair.

$\mu1(E)$ = Water attenuation coefficient at E.

$\mu 2(E)$ = Iodine attenuation coefficient at E.

4. Statistical analysis

Categorical baseline characteristics were expressed as numbers and percentages and compared between the tumors using the Fisher's exact test. Continuous variables were expressed as means and standard deviations and were compared with independent samples t-test or Mann Whitney test. Agreement between the two reviewers regarding the mean CT number and iodine concentration values was analyzed by the Bland-Altman method. *P*-values of less than 0.05 were considered statistically significant. All statistical analyses were performed with statistical software (SPSS, version 20.0, SPSS, Chicago, IL; and MedCalc, version 12.7.5, MedCalc, Mariakerke, Belgium).

III. RESULTS

The demographics and baseline clinical characteristics of the 38 patients are summarized in Table 1. In comparison of cyst and mass, male to female ratio was lower in the cyst group (1:8, 12.5%) than mass group (13:17, 56.7%). Other clinical characteristics including age, smoking,

BMI, and underlying disease were not significantly different between two groups.

Of the 38 mediastinal tumors, 8 (20.5%) were cysts and 30 (79.5%) were solid masses. The cysts consisted of thymic cysts (n=4), bronchogenic cyst (n=1), mesothelial cyst (n=1), and cystic teratomas (n=2). The solid masses consisted of thymic tumors (n=17; histological type A (n=1), AB (n=9), type B1 (n=1), and type B2 (n=1), and thymic carcinomas (n=5), respectively), schwannomas (n=6), lymphomas (n=4), small cell carcinomas (n=2), and choriocarcinoma (n=1). The final diagnoses were based on the pathological results. Thirty-one tumors were confirmed through surgical excision, six tumors were confirmed through gun biopsy, and one tumor was confirmed through surgical biopsy. Benign tumors (n=18) included 12 thymomas (type A, type AB, type B1, and type B2) and 6 schwannomas. Malignant tumors (n=12) included 5 thymic carcinomas, 4 lymphomas, 2 small cell carcinomas, and a choriocarcinoma.

Table 1. Demographic and baseline characteristics of the 38 patients

	Cysts (n=8)	Masses (n=30)	*p*-Value	Masses (n=30)		*p*-Value
				Benign (n=18)†	Malignant (n=12)‡	
Gender			**0.045**			0.141
Male	1 (12.5%)	17 (56.7%)		8 (44.4%)	9 (75%)	
Female	7 (87.5%)	13 (43.3%)		10 (55.6%)	3 (25%)	
Age (years)	44.0 ± 15.2	47.0 ± 14.5	0.631	46.3 ± 11.4	48.0 ± 18.7	0.756
Smoking			0.144			0.194
Never smoker	8 (100%)	18 (60.0%)		13 (72.2%)	5 (41.7%)	
Ex-smoker	0	6 (20.0%)		2 (11.1%)	4 (33.3%)	
Current smoker	0	6 (20.0%)		3 (16.7%)	3 (25.0%)	
BMI (kg/m2)	23.4 ± 3.3	24.1 ± 2.7	0.668	24.3 ± 3.3	23.7 ±1.6	0.524
Underlying disease	3 (37.5%)	3 (10%)	0.094	2 (11.1%)	1 (8.3%)	1.000
Hypertension	0	2 (6.7%)	1.000	1 (5.6%)	1 (8.3%)	1.000
DM	0	3 (10%)	1.000	2 (11.1%)	1 (8.3%)	1.000
Pulmonary TB	0	2 (6.7%)	1.000	2 (11.1%)	0	0.503
Myasthenia gravis						

Note: Values are mean ± standard deviation or patient number with (%)

BMI indicates body mass index; TB, tuberculosis

† 6 schwannomas, 1 thymoma (A), 9 thymomas (AB), 1 thymoma (B1), 1 thymoma (B2)

‡ 4 lymphomas, 5 thymic carcinomas, 2 small cell carcinomas, 1 choriocarcinoma

The qualitative analysis of DECT for benign and malignant mediastinal tumors are listed in Table 2. The mean diameter of benign mediastinal tumors was 48.1 ± 26.5 mm, while that of malignant mediastinal tumor was 85.0 ± 41.0 mm, with a statistically significant difference ($p = 0.013$). Contour was different between benign and malignant tumors ($p < 0.001$). Malignant mediastinal tumor had a tendency to have lobulated or irregular margin, while benign mediastinal tumor had a tendency to have smooth margin. Necrotic or cystic component was more frequent in the malignant mediastinal tumors ($p = 0.024$). Malignant mediastinal tumors had more frequent local invasion ($p < 0.001$), metastasis ($p = 0.018$), and lymphadenopathy ($p < 0.001$).

Table 2. Qualitative analysis of dual-energy CT for benign and malignant mediastinal tumors

	Benign (n=18)†	Malignant (n=12)‡	*p*-Value
Size (mean ± sd, mm)	48.1 ± 26.5	85.0 ± 41.0	**0.013**
Location			
Anterior	13 (72.2%)	12 (100%)	0.066
Middle	0	0	
Posterior	5 (27.8 %)	0	
Internal characteristics			
Contour			**<0.001**
Smooth	11 (61.1%)	0	
Lobulated	7 (38.9%)	4 (33.3%)	
Irregular	0	8 (66.7%)	
Necrotic or cystic component	5 (27.8%)	9 (75.0%)	**0.024**
Calcification	4 (22.2%)	0	0.130
External characteristics			
Local invasion	0	9 (75%)	**<0.001**
Metastasis	0	4 (33.3%)	**0.018**
Effusion	1 (5.6%)	4 (33.3%)	0.128
absent	17 (94.4%)	8 (66.7%)	
pleural	1 (5.6%)	2 (16.7%)	
pericardial	0	1 (8.3%)	
both	0	1 (8.3%)	
Lymphadenopathy	0	9 (75%)	**<0.001**

Note: Values are mean ± standard deviation or patient number with (%)

† 6 schwannomas, 1 thymoma (A), 9 thymomas (AB), 1 thymoma (B1), 1 thymoma (B2)

‡ 4 lymphomas, 5 thymic carcinomas, 2 small cell carcinomas, 1 choriocarcinoma

The quantitative analysis was performed to compare 1) cysts and masses; 2) benign and malignant masses; and 3) thymomas and thymic carcinomas (Tables 3-5). In comparison of mediastinal cysts and masses, the mean attenuation values in HU, iodine-related HU, and iodine concentration were higher in mediastinal masses than cysts (all $p < 0.001$). In comparison of benign and malignant tumors, the iodine-related HU was significantly lower in malignant tumors than benign tumors ($p = 0.041$). However, the mean attenuation values in HU and iodine concentration measurements were not significantly different between benign and malignant tumors. In comparison of thymomas and thymic carcinomas, the mean attenuation values in HU and iodine concentration measurements were significantly lower in thymic carcinomas than thymomas ($p = 0.029$ and 0.019, respectively).

Table 3. Comparison of quantitative measurements between cysts and masses

	Cysts (n=8)	Masses (n=30)	*p*-Value
Mean			
HU[a]	26.03 ± 18.14	58.40 ± 19.31	**<0.001**
IHU[b]	2.74 ± 1.73	21.62 ± 13.73	**<0.001**
IC[c]	0.20 ± 0.15	1.23 ± 0.66	**<0.001**

[a] Mean CT attenuation value in Hounsfield units.

[b] Iodine-related HU (IHU) was calculated as follows: IHU = post-enhanced HU − non-enhanced HU.

[c] Iodine concentration on the iodine (water) images (mg/ml).

Table 4. Comparison of quantitative measurements between benign and malignant masses

	Benign (n=18)	Malignant (n=12)	*p*-Value
Mean			
HU[a]	63.52 ± 19.44	51.99 ± 17.88	0.087
IHU[b]	26.03 ± 13.29	15.44 ± 12.04	**0.041**
IC[c]	1.39 ± 0.56	1.04 ± 0.75	0.079

[a] Mean CT attenuation value in Hounsfield units.

[b] Iodine-related HU (IHU) was calculated as follows: IHU = post-enhanced HU − non-enhanced HU.

[c] Iodine concentration on the iodine (water) images (mg/ml).

Table 5. Comparison of quantitative measurements between thymoma and thymic carcinomas

	Thymomas (n=12)	Thymic carcinomas (n=5)	*p*-Value
Mean			
HU[a]	74.31 ± 15.60	56.32 ± 23.32	**0.029**
IHU[b]	33.56 ± 12.28	16.45 ± 18.47	0.072
IC[c]	1.70 ± 0.47	0.91 ± 0.70	**0.019**

[a] Mean CT attenuation value in Hounsfield units.

[b] Iodine-related HU (IHU) was calculated as follows: IHU = post-enhanced HU − non-enhanced HU.

[c] Iodine concentration on the iodine (water) images (mg/ml).

The HU values on post-contrast CT images and iodine concentration measurements were different depending on the tumor types (Figures 2 and 3). Thymic carcinomas displayed lower HU on post-contrast images and lower iodine concentration measurements than thymomas (Figures 4 and 5). Schwannomas also displayed relatively lower value of HU on post-contrast images and iodine concentration measurements compared to thymomas. Lymphomas displayed relatively higher iodine concentration measurements compared to HU values. Choriocarcinoma demonstrated lower value of HU on post-contrast images and iodine concentration measurements compared to other solid masses.

The results of Bland-Altman analysis of agreement between the HU values and iodine concentration for the two reviewers are shown in Figure 6. The mean difference between the HU values assigned by the two reviewers was 0.5 HU (95% Confidence interval (CI): -7.8 HU, 8.8 HU). The mean difference of the iodine concentration values between the two reviewers was 0.02 mg/ml (95% CI: -0.16 mg/ml, 0.20 mg/ml).

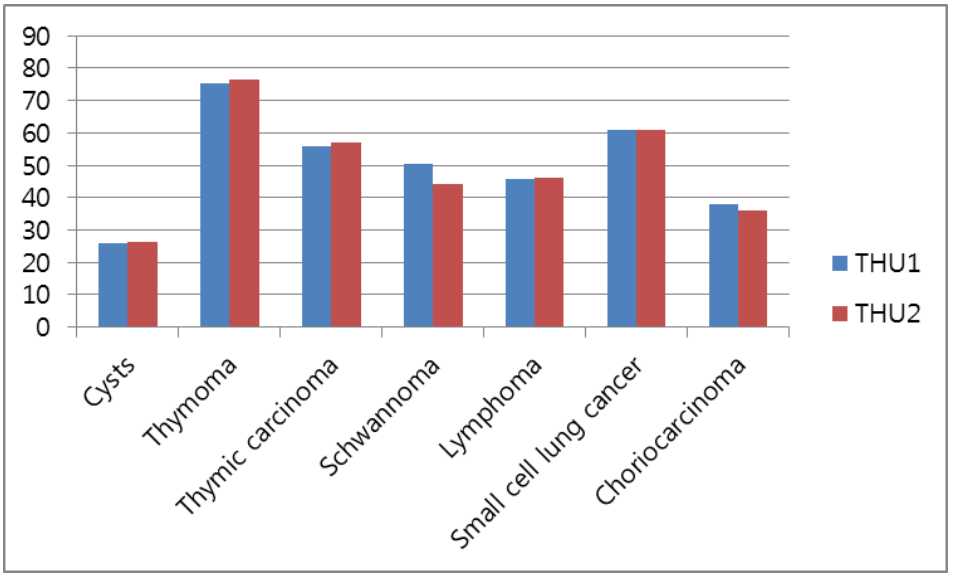

Figure 2A. HU value measurements for mediastinal tumors by two reviewers. THU1: the mean attenuation value (Hounsfield units (HU)) measurement by reviewer 1, THU2: the mean attenuation value (Hounsfield units (HU)) measurement by reviewer 2.

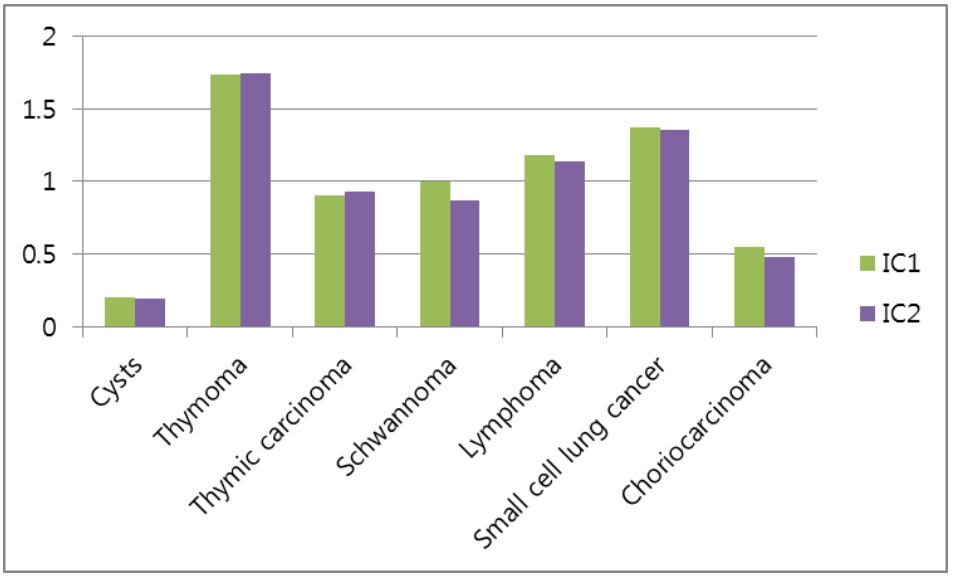

Figure 2B. Iodine concentration measurements for mediastinal tumors by two reviewers. IC1: Iodine concentration measurement by reviewer 1, IC2: Iodine concentration measurement by reviewer 2

(A) (B)

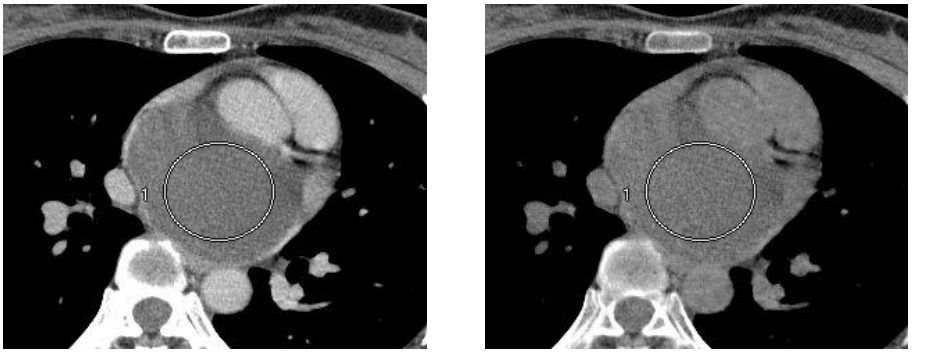

(C)

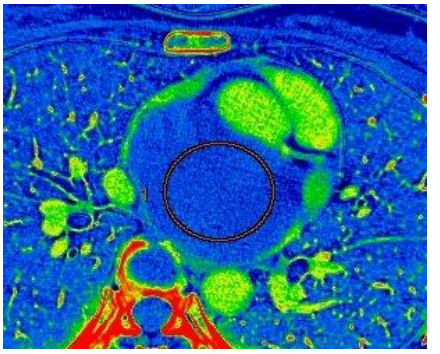

Figure 3. Dual-energy computed tomography (DECT) images in a 41-year old woman whose tumor was confirmed to be a bronchogenic cyst. (A) The contrast-enhanced CT image obtained from DECT data shows middle mediastinal tumor; the mean attenuation value measured 22.2 Hounsfield units (HU). (B) On MSI image representing pre-contrast CT image, non-enhanced HU measured 20.4 HU. The iodine-related HU becomes 1.8 HU. (C) On the iodine (water) image, the mean iodine concentration within the ROI was 0.097 mg/ml.

(A) (B)

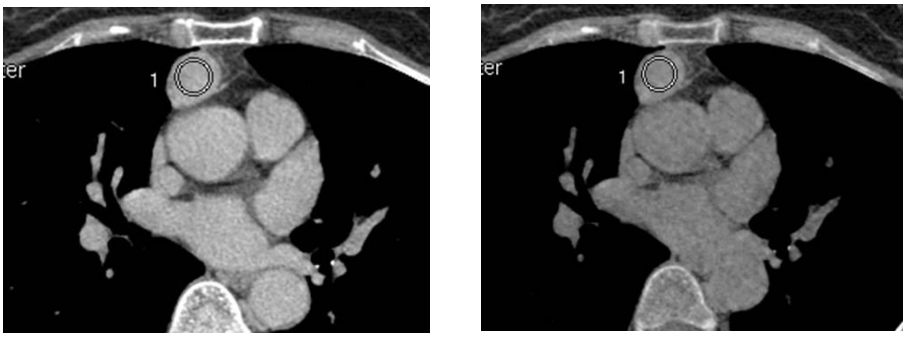

(C)

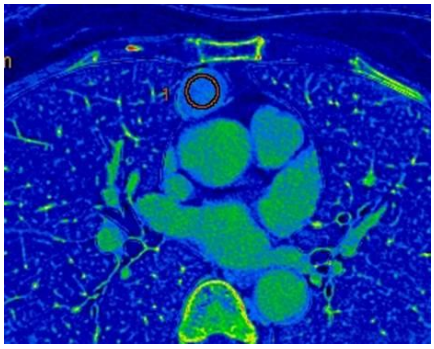

Figure 4. Dual-energy computed tomography (DECT) images in a 59-year old woman whose tumor was confirmed to be a thymoma, type AB. (A) The contrast-enhanced CT image obtained from DECT data shows an anterior mediastinal tumor; the mean attenuation value measured 102.6 Hounsfield units (HU). (B) On MSI image representing pre-contrast CT image, non-enhanced HU measured 51.8 HU. The iodine-related HU becomes 50.8 HU. (C) On the iodine (water) image, the mean iodine concentration within the ROI was 2.356 mg/ml.

(A) (B)

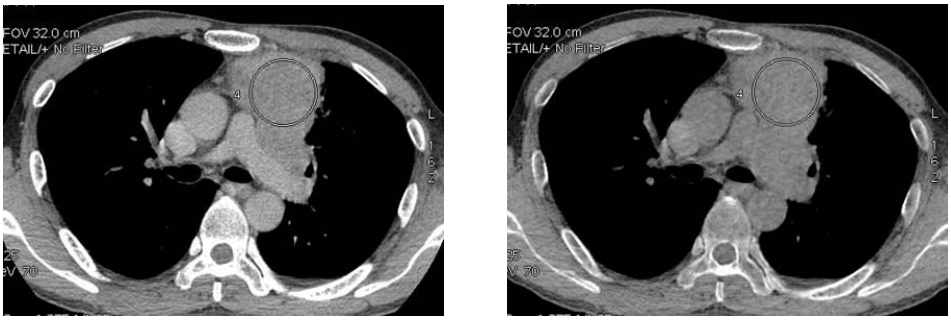

(C)

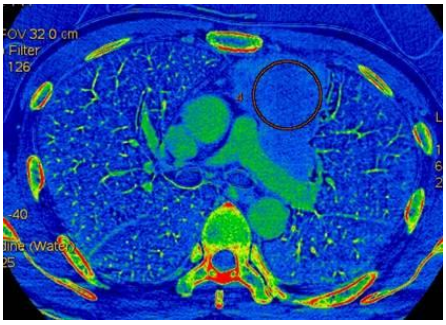

Figure 5. Dual-energy computed tomography (DECT) images in a 53-year old man whose tumor was confirmed to be a thymic carcinoma. (A) The contrast-enhanced CT image obtained from DECT data shows an anterior mediastinal tumor; the mean attenuation value measured 56.0 Hounsfield units (HU). (B) On MSI image representing pre-contrast CT image, non-enhanced HU measured 44.9 HU. The iodine-related HU becomes 11.1 HU. (C) On the iodine (water) image, the mean iodine concentration within the ROI was 0.752 mg/ml.

(A)

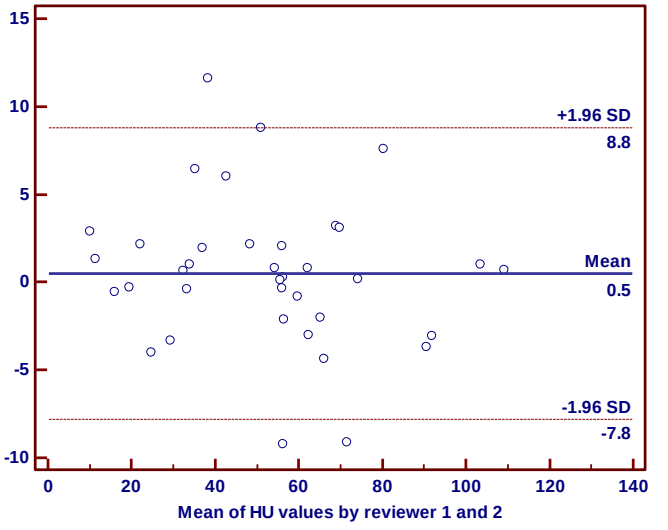

Figure 6A. Result of Bland-Altman analysis. Graph shows attenuation values measured by two reviewers (mean difference 0.5 Hounsfield units (HU); 95% CI, -7.8 to 8.8 HU).

(B)

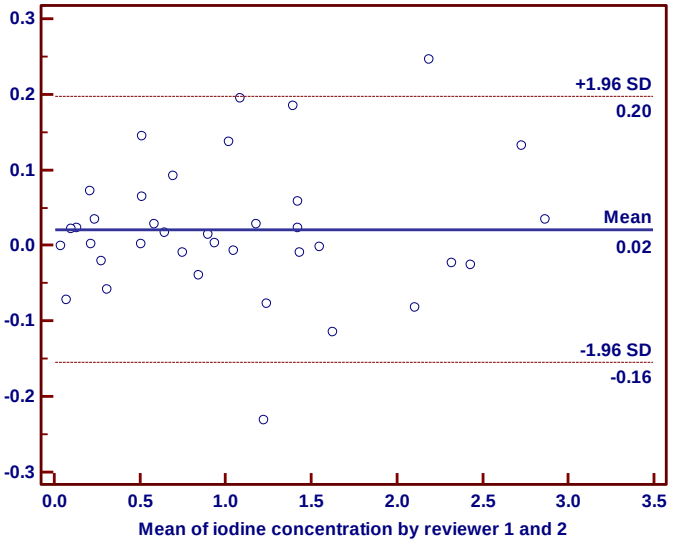

Figure 6B. Result of Bland-Altman analysis. Graph shows iodine concentration values measured by two reviewers (mean difference 0.02 mg/ml; 95% CI, -0.16 to 0.20 mg/ml).

IV. DISCUSSION

This study was designed to show that DECT would provide a more reliable quantitative parameter to indicate tumor enhancement with iodine concentration measurements in the differentiation of mediastinal tumors. To achieve the objectives, we measured the HU on post-contrast images, iodine-related HU, and iodine concentration of the mediastinal tumors and compared those values between cysts and solid mediastinal tumors, and between benign and malignant mediastinal tumors. Our results suggest that iodine-related HU and iodine concentration obtained from the DECT data can be a feasible quantitative parameter for differentiation of mediastinal tumors.

Cysts comprise 15-20% of all mediastinal masses.[19] There are various types of mediastinal cysts including bronchogenic cysts, esophageal duplication cysts, pericardial cysts, neurenteric cysts, meningocele, thymic cysts, cystic teratoma, and lymphangioma. Characterization of these cystic lesions may at times be difficult owing to the variable composition of fluid and associated complications such as hemorrhage or infection, and these cystic lesions may be mistaken for solid lesions.[6] A conservative approach can be considered for small, asymptomatic

mediastinal cysts and surgical excision offers definite cure for symptomatic cysts with low morbidity and mortality rates.[20] As cysts and masses have different treatment options, accurate diagnosis is required.

For differentiation of cysts and masses, all three values including HU on post-contrast images, iodine-related HU, and iodine concentration were significantly different between two groups. Two thymomas (type AB) in our study demonstrated very high attenuation (higher than 100 HU) on post-contrast images, which increased the mean HU values of the masses.

Bronchogenic cysts can manifest as soft-tissue attenuation masses on CT scans and differentiation from solid lesions can be problematic.[21] As CT number merely represents different density levels of tissues and other substances, HU values measured on post-contrast images can be influenced by not only iodine contrast delivered by the vascular system, but also by the presence of dense material such as blood, protein or calcification. In the current study, we had only one case of bronchogenic cyst and we did not separate the bronchogenic cyst and other cysts for subgroup analysis in this study. However, we believe that DECT with iodine concentration measurement can help in the differentiation between soft-tissue attenuation cyst and solid mass. Further study with larger

sample size is recommended to confirm the usefulness of DECT for differentiation between soft-tissue attenuation cysts and masses.

In comparison of benign and malignant mediastinal tumors, iodine-related HU was significantly different between two groups, while HU on post-contrast images or iodine concentration measurements were not significantly different. Previous study on DECT for differentiation of benign and malignant mediastinal tumors revealed that iodine concentration measurements were significantly higher in malignant tumor groups while mean attenuation values were not significantly different.[22] In our study, iodine-related HU was significantly higher in benign tumor groups compared to malignant tumor groups, which is not consistent with previous study. Different results may be caused by different sample groups of heterogeneous tumor types with different characteristics. Achieving a simple quantitative parameter for the differentiation of benignity and malignancy within this heterogeneous group was challenging. In subgroup analysis, schwannomas and lymphomas showed similar attenuation values on post contrast CT images, whereas lymphomas showed higher iodine concentration measurements compared to schwannomas. This result suggests that a DECT technique have a potential to provide additional diagnostic

information in differentiating between various tumor groups in the mediastinum. DECT allows selective quantification and visualization of iodine concentration or iodine-related HU differences by generating the material suppressed iodine image also known as the virtually nonenhanced image without the need for an additional CT scanning for noncontrast image. Therefore a single-phase scanning might allow for characterization of mediastinal masses with the use of DECT, and omitting of a nonenhanced acquisition can reduce radiation exposure to patients.

Additionally, we investigated the DECT capability in the differentiation among thymic epithelial tumors. Thymic epithelial tumors are the most common tumor in the anterior mediastinum, accounting for 30% of all masses in this anatomical region in adults and 20% of all mediastinal masses regardless of compartmental location.[23] The most commonly used classification is from the World Health Organisation (WHO), which was developed in 1999 and revised in 2004. This classification distinguishes thymomas on the basis of the prevalence of the cellular subpopulation present, and this classification reflects both the clinical and functional features of thymic epithelial tumors and thus contributes to the clinical assessment and treatment of patients with these tumors.[24-26] In our results,

thymic carcinomas displayed significantly lower HU on post-contrast images and iodine concentration. This result may be explained by frequent necrotic change in this tumor group.

We acknowledge that this study had several limitations. First, we included 38 patients with heterogeneous mediastinal tumors, and the sample size is too small for subgroup analysis. Achieving a simple quantitative parameter to represent tumor character within this heterogeneous group was challenging. Second, the contrast injection protocol may have had a significant influence on the results. In prior studies, malignant lung nodules have shown peak enhancement between 1 and 2 minutes after the administration of contrast material.[11,14] Therefore, we set up the scan to begin 60 seconds after peak enhancement of the main PA. Accordingly, CT images were acquired in the phase between 1 and 2 minutes after contrast injection as we sought to obtain images of malignant mediastinal tumors showing peak enhancement. However, various tumors with heterogeneous features may have different enhancement pattern and our injection protocol may not always have us obtain images of mediastinal tumors with their peak enhancement. Finally, another limitation of this study is that DECT imparts an unnecessarily higher radiation dose. The dual-energy

technique utilizes the acquisition of two data sets at different energy levels, inevitably leading to greater radiation exposure to patients.

V. CONCLUSION

DECT using a quantitative analytic method based on iodine concentration measurements can be used to evaluate tumor enhancement of mediastinal tumors using a single-phase scanning. Therefore, we believe that DECT could be a helpful complementary tool in cases where conventional contrast CT is inconclusive. Further studies with larger sample size will further refine and contribute to the diagnostic information available of DECT for differentiating mediastinal tumors.

REFERENCES

1. Whitten CR, Khan S, Munneke GJ, Grubnic S. A diagnostic approach to mediastinal abnormalities. *Radiographics : a review publication of the Radiological Society of North America, Inc.* May-Jun 2007;27(3):657-71.
2. Maisch B, Seferovic PM, Ristic AD, et al. Guidelines on the diagnosis and management of pericardial diseases executive summary; The Task force on the diagnosis andmanagement of pericardial diseases of the European society of cardiology. *European heart journal.* Apr 2004;25(7):587-610.
3. Gulluoglu MG, Kilicaslan Z, Toker A, Kalayci G, Yilmazbayhan D. The diagnostic value of image guided percutaneous fine needle aspiration biopsy in equivocal mediastinal masses. *Langenbeck's archives of surgery /Deutsche Gesellschaft fur Chirurgie.* Jun 2006;391(3):222-7.
4. Mikhail M, Mekhail Y, Mekhail T. Thymic neoplasms: a clinical update. *Current oncology reports.* Aug 2012;14(4):350-8.

5. Takahashi K, Al-Janabi NJ. Computed tomography and magnetic resonance imaging of mediastinal tumors. *Journalof magnetic resonance imaging : JMRI.* Dec 2010;32(6):1325-39.

6. Jeung MY, Gasser B, Gangi A, et al. Imaging of cystic masses of the mediastinum. *Radiographics : a review publication of the Radiological Society of North America,Inc.* Oct 2002;22 Spec No:S79-93.

7. Erasmus JJ, McAdams HP, Donnelly LF, Spritzer CE. MR imaging of mediastinal masses. *Magn Reson Imaging Clin N Am.* Feb 2000;8(1):59-89.

8. Gumustas S, Inan N, Sarisoy HT, et al. Malignant versus benign mediastinal lesions: quantitative assessment with diffusion weighted MR imaging. *European radiology.* Nov 2011;21(11):2255-60.

9. Fox SB, Gatter KC, Harris AL. Tumour angiogenesis. *J Pathol.* Jul 1996;179(3):232-7.

10. Tomita M, Matsuzaki Y, Edagawa M, et al. Correlation between tumor angiogenesis and invasiveness in thymic epithelial tumors. *J Thorac Cardiovasc Surg.* Sep 2002;124(3):493-8.

11. Zhang M, Kono M. Solitary pulmonary nodules: evaluation of blood flow patterns with dynamic CT. *Radiology.* Nov 1997;205(2):471-8.

12. Yamashita K, Matsunobe S, Tsuda T, et al. Solitary pulmonary nodule: preliminary study of evaluation with incremental dynamic CT. *Radiology.* Feb 1995;194(2):399-405.

13. Swensen SJ, Viggiano RW, Midthun DE, et al. Lung nodule enhancement at CT: multicenter study. *Radiology.* Jan 2000;214(1):73-80.

14. Yi CA, Lee KS, Kim EA, et al. Solitary pulmonary nodules: dynamic enhanced multi-detector row CT study and comparison with vascular endothelial growth factor and microvessel density. *Radiology.* Oct 2004;233(1):191-9.

15. Jeong YJ, Lee KS, Jeong SY, et al. Solitary pulmonary nodule: characterization with combined wash-in and washout features at dynamic multi-detector row CT. *Radiology.* Nov 2005;237(2):675-83.

16. Lee KS, Yi CA, Jeong SY, et al. Solid or partly solid solitary pulmonary nodules: their characterization using contrast wash-in

and morphologic features at helical CT. *Chest.* May 2007;131(5):1516-25.

17. Chae EJ, Song JW, Krauss B, et al. Dual-energy computed tomography characterization of solitary pulmonary nodules. Journal of thoracic imaging. Nov 2010;25(4):301-10.

18. Johnson TR, Krauss B, Sedlmair M, et al. Material differentiation by dual energy CT: initial experience.*European radiology.* Jun 2007;17(6):1510-7.

19. Oldham HN, Jr. Mediastinal tumors and cysts. *The Annals of thoracic surgery.* Mar 1971;11(3):246-75.

20. Esme H, Eren S, Sezer M, Solak O. Primary mediastinal cysts: clinical evaluation and surgical results of 32 cases. *Texas Heart Institute journal / from the Texas Heart Institute of St. Luke's Episcopal Hospital, Texas Children's Hospital.* 2011;38(4):371-4.

21. McAdams HP, Kirejczyk WM, Rosado-de-Christenson ML, Matsumoto S. Bronchogenic cyst: imaging features with clinical and histopathologic correlation. *Radiology.* Nov 2000;217(2):441-6.

22. Lee SH, Hur J, Kim YJ, Lee HJ, Hong YJ, Choi BW. Additional value of dual-energy CT to differentiate between benign and

malignant mediastinal tumors: An initial experience. *European journal of radiology.* Nov 2013;82(11):2043-9.

23. Priola AM, Priola SM, Cardinale L, Cataldi A, Fava C. The anterior mediastinum: diseases. *La Radiologia medica.* Apr 2006;111(3):312-42.

24. Chalabreysse L, Roy P, Cordier JF, Loire R, Gamondes JP, Thivolet-Bejui F. Correlation of the WHO schema for the classification of thymic epithelial neoplasms with prognosis: a retrospective study of 90 tumors. *The American journal of surgical pathology.* Dec 2002;26(12):1605-11.

25. Travis WD, World Health Organization., International Agency for Research on Cancer., International Association for theStudy of Lung Cancer., International Academy of Pathology. *Pathology and genetics of tumours of the lung, pleura, thymus and heart.* Lyon, Oxford: IARC Press, Oxford University Press (distributor); 2004.

26. Jeong YJ, Lee KS, Kim J, Shim YM, Han J, Kwon OJ. Does CT of thymic epithelial tumors enable us to differentiate histologic subtypes and predict prognosis? *AJR. American journal of roentgenology.* Aug 2004;183(2):283-9.

ABSTRACT(IN KOREAN)

종격동 종양의 감별에 대한 이중에너지컴퓨터단층촬영의 유용성

<지도교수 허진>

연세대학교 대학원 의학과

장 수 연

목적: 종격동의 낭성종괴와 고형종괴의 감별, 그리고 종격동의 양성종양과 악성종양의 감별에서 이중에너지컴퓨터단층촬영의 진단적 유용성을 평가한다.

대상 및 방법: 본 전향적 연구는 임상시험심사위원회의 승인 및 환자들의 사전 동의 하에 진행되었다. 흉부단순촬영이나 흉부컴퓨터단층촬영에서 종격동 종양이 의심되는 38명의 환자들이 gemstone spectral imaging (GSI) mode (GE HD750)를

이용한 이중에너지컴퓨터단층촬영을 시행 받았다 (남자 18명, 평균 연령 46세). 정성적 분석을 위해 각 종괴의 크기, 위치, 내적 특성 및 외적 특성을 분석하였고, 정량적 분석을 위해 두 명의 영상의학과 의사가 감쇠음영, 요오드 관련 감쇠음영, 요오드 농도를 측정하였다. 최종 진단은 병리학적 결과를 이용하였다. 통계학적 분석은 Fisher's exact test, independent samples t-test, Mann-Whitney test 를 사용하였다.

결과: 정성적 분석 결과 악성 종양의 경우 양성 종양보다 크기가 크고 ($p = 0.015$), 소엽상 또는 불규칙한 윤곽을 보였으며 ($p < 0.001$), 괴사된 부위 ($p = 0.025$)가 흔하였고, 국소적 침범 ($p < 0.001$)이나 원격 전이 ($p = 0.016$), 림프절 종대 ($p < 0.001$) 소견들이 흔하였다. 정량적 분석 결과 고형종괴가 낭종보다 높은 감쇠음영, 요오드 관련 감쇠음영, 요오드 농도를 보였다 (모두 $p < 0.001$). 양성종양과 악성종양을 비교시 양성종양이 악성종양 보다 높은 요오드 관련 감쇠음영을 보였다 ($p = 0.041$).

결론: 이중에너지컴퓨터단층촬영은 요오드 농도를 정량적으로

측정함으로써 비조영시기의 영상 촬영 없이 한 번의 영상 촬영으로 종격동 종양의 조영증강 정도를 평가할 수 있다. 따라서 고전적인 조영증강 컴퓨터단층촬영으로 감별이 어려운 종격동 종양의 경우 이중에너지컴퓨터단층촬영이 추가적인 진단 도구로 유용하게 사용될 수 있을 것이다.

핵심되는 말: 종격동 신생물, 이중에너지컴퓨터단층촬영, 감별, 양성 종양, 악성 종양, 낭종